

DENOISING SONAR IMAGES

Alexandru ISAR*, Dorina ISAR*, Ioana ADAM*

* "Politehnica" University Timisoara.

Corresponding author: Alexandru Isar, "Politehnica" University, Electronics and Telecommunications Faculty, 2 Bd. V. Parvan, 1900 Timisoara, Romania, fax: 0256403295, tel.:025640307, e-mail: alexandru.isar@etc.utt.ro

Abstract. The SONAR images are perturbed by speckle noise. The despecklisation is necessary to optimize the image understanding. This paper presents, starting from a denoising method proposed by Donoho, a new filtering procedure, applied in the Double Tree Discrete Wavelet Transform domain. This technique reduces the noise without affecting the discontinuities. Some simulation examples prove the performances of the new denoising method.

Key words: Denoising; SONAR images; MAP filtering; Double Tree Discrete Wavelet Transform.

1. INTRODUCTION

The SONAR systems are used in a large spectrum of military or civil applications. The user is able to distinguish a number of different regions, analyzing a SONAR image. This classification process is sometimes very difficult, due to the presence of the speckle. The use of anti-speckle filters is required before the application of a detection or classification procedure. Such a filter must realize an important speckle reduction in the regions where the sonar reflectivity is constant and a conservation of the textures and other structures of the seafloor image in the other regions. Some classical estimators are:

- The Kuan's filter (linear estimator who minimizes the mean squared estimation error);
- The Frost's filter (Wiener filter matched to multiplicative noise), [1].

Between the modern estimators can be found:

- The marginal Maximum A Posteriori, MAP, filter (who maximizes the a posteriori probability),
- The multi-resolution MAP filter (who minimizes the Min-Max estimation error), [2].

Initially those estimators have used analysis windows with constant dimensions. Next, these dimensions were chosen adaptively, taking into account local aspects of the acquired image, [3]. A new category of modern estimators utilizes the wavelets theory, [2], [4], [5].

2. THE NEW DENOISING METHOD

The SONAR images, $i_r(x, y)$, are affected by a multiplicative noise, called speckle, $br(x, y)$, $i_r = i_o \cdot br$. When the speckle is entirely developed, the hypothesis of independence of random processes $i_o(x, y)$ and $br(x, y)$ can be adopted [4]. The structure of the denoising system proposed is presented in figure 1.

The Double Tree Discrete Wavelet Transform, DTDWT, [6], is applied after the transformation of the multiplicative noise into an additive one, realized by the logarithm computation block from figure 1. The result of this transformation is processed using a MAP filter, of bishrink type, [7]. At the system output, after the computation of the inverse DTDWT, IDTDWT, and the logarithm inversion, the estimation of the useful component of the input image, $\hat{i}_o(x, y)$, can be measured. Because the logarithm computation block modifies the mean of the useful component of the input image, it must be restored after the logarithm inversion. This is the reason why the architecture of the system in figure 1 was completed with the blocks for mean

extraction and mean correction. The first one extracts the mean of the input image. Because the mean of the multiplicative noise is unitary, the value extracted is equal with the mean of the useful part of the input image. The mean correction block rejects the mean of the signal obtained at the output of the logarithm inversion system and adds to the result the mean of the useful component of the input image, furnished by the mean extraction block.

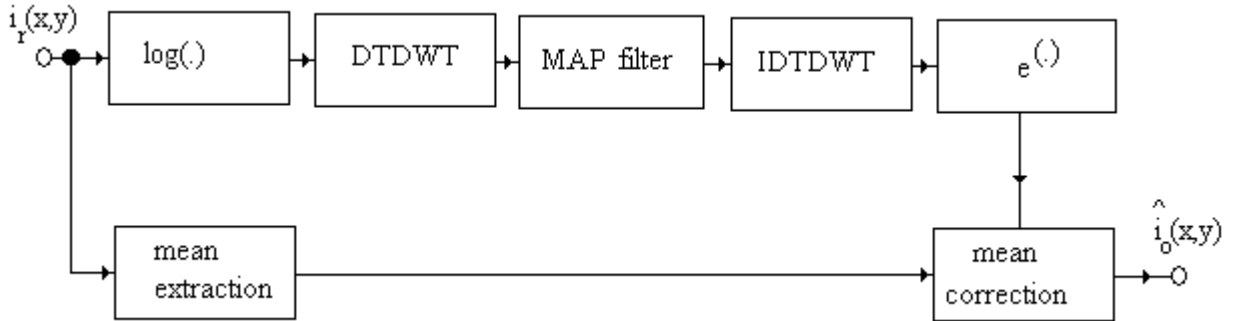


Figure 1. The proposed denoising system.

3. STATISTICAL ANALYSIS

This analysis will be made tacking into account each block from figure 1.

3.1. The noise component of the acquired image

The SONAR images are a particular case of Synthetic Aperture Radar, SAR, images. The speckle that perturbs the SAR images is a white noise distributed following a law Gamma, which parameter is the number of views, L , [4]:

$$f_{X_\Gamma}(x) = \frac{L^L}{\Gamma(L)} \cdot x^{L-1} \cdot e^{-Lx} \quad \text{for } x \geq 0. \quad (1)$$

where Γ represents the Euler's Gamma function:

$$\Gamma(L) = \int_0^{\infty} t^{L-1} \cdot e^{-t} dt. \quad (2)$$

The speckle's mean is given by:

$$\mu_\Gamma = 1, \quad (3)$$

and its variance by:

$$\sigma_\Gamma^2 = E[X_\Gamma^2] - \mu_\Gamma^2 = \frac{L(L+1)}{L^2} - 1 = \frac{1}{L}. \quad (4)$$

The random variable X_Γ is transformed obtaining the random variable $Y_{\log-\Gamma}$, which describes the speckle noise at the input of the second block, in accordance with the change of variable realized by the first block in figure 1. The relation between the probability density functions, pdfs, of these two random variables is:

$$f_{Y_{\log-\Gamma}}(y) = \left. \frac{f_{X_{\Gamma}}(x)}{\left| \frac{dy}{dx} \right|} \right|_{x=e^y} = \frac{\frac{L^L}{\Gamma(L)} x^{L-1} e^{-Lx}}{\frac{1}{x}} \bigg|_{x=e^y} = \frac{L^L}{\Gamma(L)} x^L e^{-Lx} \bigg|_{x=e^y} = \frac{L^L}{\Gamma(L)} e^{Ly} e^{-Le^y}. \quad (5)$$

The value of the mean of the law log-Gamma is given by:

$$\mu_{\log-\Gamma} = \sum_{k=1}^{L-1} \frac{1}{k} - \gamma - \ln L, \quad (6)$$

where γ represents the Euler's number. Its variance is:

$$\sigma_{\log-\Gamma}^2 = \frac{\pi^2}{6} - \sum_{k=1}^{L-1} \frac{1}{k^2}. \quad (7)$$

So, the noise that perturbs the logarithm of the useful part of the SAR image is white and distributed following a law log-Gamma whose statistical characteristics are given by the relations (5), (6) and (7). The SONAR images are a particular case of SAR images, obtained for $L = 1$. In this case the law Γ becomes a law χ^2 . After the logarithm computation, a law $\log-\chi^2$ is obtained. Its pdf is:

$$f_{\log-\chi^2}(y) = e^y \cdot e^{-e^y}. \quad (8)$$

The value of its mean is:

$$\mu_{\log-\chi^2} = -\gamma, \quad (9)$$

and the value of its variance is:

$$\sigma_{\log-\chi^2}^2 = \frac{\pi^2}{6}. \quad (10)$$

3.2. The DTDWT statistical analysis

There are many wavelet transforms, WTs, used in denoising applications. The first WT used in this kind of applications was the Discrete Wavelet Transform, DWT, a non-redundant transform. It has three disadvantages for image processing: it is not translation invariant; it has a poor directional selectivity; and the results obtained after its application are very sensitive to the selection of its parameters. It has two parameters: the mother wavelets, MW and the primary resolution, PR, (number of iterations). Another WT used in denoising applications is the Diversity Enhanced Discrete Wavelet Transform, DEDWT. It has a controlled redundancy and is insensitive to the parameter selection. It is not translation invariant and its directional selectivity is poor. Another WT used in denoising applications is the Undecimated Discrete Wavelet Transform, UDWT. This is a very redundant WT. It is translation invariant but its directional selectivity is also poor. The DTDWT is redundant. Its redundancy is of 4. It is almost translation invariant and it has a good directional selectivity. Those are the reasons to select this WT for the system described in this paper.

3.2.1. The DTDWT

The 1D implementation of this transform, represented in figure 2, is made of two trees. Each tree computes a Discrete Wavelet Transform, DWT, [8]. The mother wavelets used for the computation of the DWT corresponding to the second tree is the Hilbert transform of the mother wavelets used for the computation of the DWT corresponding to the first tree. In figure 2 are represented three iterations of the DTDWT. Each tree represents a DWT. Each cell of the tree, corresponding to an iteration of the DWT, is composed of two filters and of two sub-samplers. The filter with the impulse response m_0 (corresponding to

a scaling function) is a low-pass one and the filter with the impulse response m_1 (corresponding to a MW) is a high-pass one. They form a quadrature mirror filters pair (the MW is build with the aid of the corresponding scaling function). The statistical analysis of the DTDWT is based on the statistical analysis of the DWT. This is the reason why in the following pages the DWT will be analyzed first.

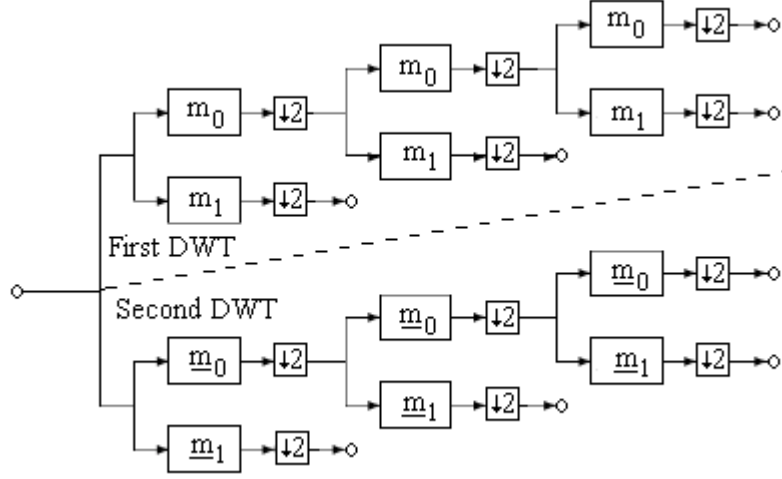


Figure 2. The one-dimensional DTDWT computation system.

3.2.2. The DWT statistical analysis

An iteration of the 2D DWT of an image is realized by the system presented in figure 3. The input image represents the approximation sub-image, ${}_x D_{m-1}^4$, obtained at the previous, $(m-1)$, iteration. The approximation, ${}_x D_m^4$ and detail, ${}_x D_m^3$, ${}_x D_m^2$ and ${}_x D_m^1$ sub-images are obtained at the outputs of the computation system. The first iteration input image is the image of the logarithm of the acquired SONAR image, ${}_x D_0^4$. The coefficients of the 2D DWT, corresponding to a sub-image, can be computed using the following relation:

$${}_x D_m^k [n, p] = \langle x(\tau_1, \tau_2), \Psi_{m,n,p}^k(\tau_1, \tau_2) \rangle \quad k = \overline{1,4}. \quad (11)$$

where the mother wavelets can be factorized with the aid of the product:

$$\Psi_{m,n,p}^k(\tau_1, \tau_2) = \alpha_{m,n,p}^k(\tau_1) \cdot \beta_{m,n,p}^k(\tau_2), \quad (12)$$

and the two factors can be computed with the aid of the scaling function $\phi(\tau)$ and of the MW $\psi(\tau)$, using the following relations, [9]:

$$\phi_{m,n}(\tau) = 2^{-\frac{m}{2}} \phi(2^{-m} \tau - n) \quad \text{and} \quad \psi_{m,n}(\tau) = 2^{-\frac{m}{2}} \psi(2^{-m} \tau - n). \quad (13)$$

In the same reference is computed the pdf of the wavelet coefficients. The image x represents the sum of the logarithm of the useful image, s and the logarithm of the noise image, b :

$$x = s + b. \quad (14)$$

Because these two random processes are not correlated, the relation between the correlation functions of the corresponding wavelet coefficients is the following:

$$\Gamma_{{}_x D_m^k} = \Gamma_{{}_s D_m^k} + \Gamma_{{}_b D_m^k}. \quad (15)$$

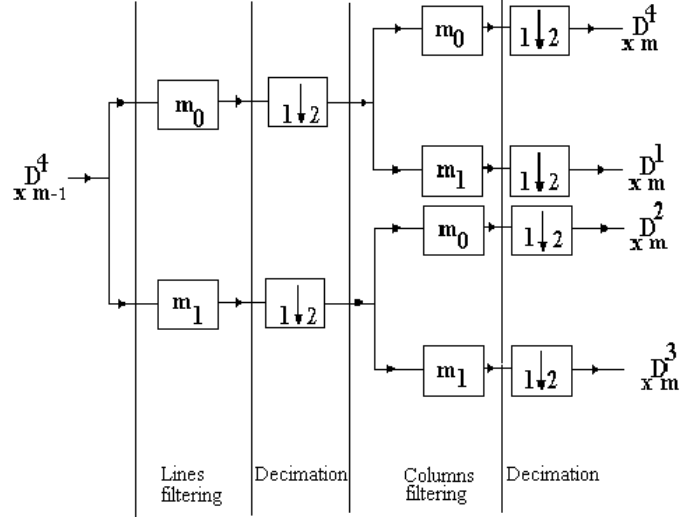


Figure 3. The 2D DWT computation system. The m 'th iteration.

The correlation function of the random variable ${}_x D_m^k[n, p]$, is given by the relation, [9]:

$$\begin{aligned} \Gamma_{{}_x D_m^k} [n_1, n_2, p_1, p_2] &= E \left\{ {}_x D_m^k [n_1, p_1] ({}_x D_m^k [n_2, p_2])^* \right\} = \\ &= \int_{R^4} E \left\{ x(\tau_1, \tau_2) x^*(\tau_3, \tau_4) \right\} \cdot \Psi_{m, n_1, p_1}^k(\tau_1, \tau_2) \cdot \Psi_{m, n_2, p_2}^{k*}(\tau_3, \tau_4) d\tau_1 d\tau_2 d\tau_3 d\tau_4. \end{aligned} \quad (16)$$

or:

$$\Gamma_{{}_x D_m^k} [n_1, n_2, p_1, p_2] = \frac{1}{4\pi^2} \cdot \int_{R^2} \gamma_x(2^{-m} \mathbf{v}_1, 2^{-m} \mathbf{v}_2) \cdot \left| \mathfrak{S}_2 \{ \Psi^k \} (\mathbf{v}_1, \mathbf{v}_2) \right|^2 \cdot e^{-j[v_1(n_2 - n_1) + v_2(p_2 - p_1)]} d\mathbf{v}_1 d\mathbf{v}_2. \quad (17)$$

Tacking into account that the input noise, b , is white, of variance $\sigma_{\log-\chi^2}^2$, the power spectral density can be written:

$$\gamma_b(2^{-m} \mathbf{v}_1, 2^{-m} \mathbf{v}_2) = \sigma_{\log-\chi^2}^2, \quad (18)$$

and the 2D DWT of the noise image coefficients correlation function expression is:

$$\Gamma_{{}_b D_m^k} [n, p] = \sigma_{\log-\chi^2}^2 \cdot \delta[n] \cdot \delta[p]. \quad (19)$$

The 2D DWT of the noise image coefficient sequences are white noise sub-images having the same variance. The mother wavelets selection does not have any influence on this result. The first and second order moments of the image obtained by filtering in the DWT domain are computed in the following. The mean is given by:

$$\begin{aligned} E \{ {}_x D_m^k [n, p] \} &= E \left\{ \int_{R^2} x(\tau_1, \tau_2) \cdot \Psi_{m, n, p}^{k*}(\tau_1, \tau_2) d\tau_1 d\tau_2 \right\} = \mu_x \cdot \mathfrak{S}_2 \{ \Psi_{m, n, p}^{k*} \} (0, 0) = \\ &= \mu_x \cdot 2^m \cdot \mathfrak{S}_2 \{ \Psi^{k*} \} (0, 0) = \mu_x \cdot 2^m \cdot \mathfrak{S} \{ \alpha^{k*} \} (0) \cdot \mathfrak{S} \{ \beta^{k*} \} (0) = \begin{cases} 0, & k=1, 2, 3 \\ 2^m \cdot \mu_x, & k=4 \end{cases}. \end{aligned} \quad (20)$$

Only the mean of the approximation sub-image is not null. The 2D DWT of the noise image, b , has a mean given by:

$$E\{ {}_b D_m^k [n, p] \} = \begin{cases} 0, & k = 1, 2, 3 \\ 2^m \cdot \mu_{\log-\chi^2}, & k = 4 \end{cases} \quad (21)$$

In practice, the DWT is computed utilizing the maximal number of iterations. Then, the dimensions of the approximation sub-image are very small. This is the reason why this sub-image is not filtered. The variance of the 2D DWT of the noise image can be computed using the following relation:

$$\sigma_{{}_x D_m^k}^2 = E\{ |{}_x D_m^k [n, p]|^2 \} = \Gamma_{{}_x D_m^k} (0, 0) = \frac{1}{4\pi^2} \int_{R^2} \gamma_x(2^m v_1, 2^m v_2) \left| \mathfrak{S}_2 \{ \Psi^k \} (v_1, v_2) \right|^2 dv_1 dv_2. \quad (22)$$

The DWT of the noise image, b , has a variance given by:

$$\sigma_{{}_b D_m^k}^2 = \begin{cases} \sigma_{\log-\chi^2}^2, & k = 1, 2, 3 \\ \sigma_{\log-\chi^2}^2 - 2^{2m} \mu_{\log-\chi^2}^2, & k = 4 \end{cases} \quad (23)$$

This variance is constant for all detail sub-images. Because, for m sufficiently high:

$$\sigma_b^2 - 2^{2m} \gamma^2 \cong 0, \quad (24)$$

it can be concluded that, after some iterations, the noise contained in the approximation sub-images was completely eliminated. This is another reason to filter only the detail sub-images. Each such sub-image is modeled by a random variable whose pdf can be computed using some variable changes, starting from a random variable distributed following a law $\log-\chi^2$. Because the union of these sub-images, DWTd, with the approximation sub-image, DWTa, represents the entire DWT, the central limit theorem can be applied. This is the reason why the wavelet coefficients have asymptotically a Gaussian pdf. As all the detail sub-images are zero mean random variables, this Gaussian pdf has also a zero mean. The correlation of the 2D DWT coefficients of s is given by:

$$\Gamma_{{}_s D_m^k} [n, p] = 2^{2m} \Gamma_s [2^m n, 2^m p] \quad (25)$$

its mean by:

$$E\{ {}_s D_m^k [n, p] \} = \begin{cases} 0, & k = 1, 2, 3 \\ 2^m \cdot \mu_s, & k = 4 \end{cases} \quad (26)$$

and its variance by:

$$\sigma_{{}_s D_m^k}^2 = 2^{2m} \sigma_s^2. \quad (27)$$

The variance of the 2D DWT of the logarithm of the useful image increases when the iteration index increases. The computation of the 2D DTDWT is based on the computation of two 2D DWTs using two different mother wavelets. This is the reason why the conclusions of the statistical analysis of the 2D DWT can be applied to the statistical analysis of the 2D DTDWT.

3.3. Statistical analysis of the bishrink filter

The bishrink filter was first proposed in [7].

3.3.1. The bishrink filter

There is a certain correlation between the values of a DWT coefficient at a given scale and the same coefficient situated in the same geometrical position at the following scale (called parent of the considered coefficient), according to (17). In [7] is considered only the dependency between a coefficient (belonging to

a certain detail sub-image) and his parent. This kind of dependency is represented in figure 4. Using the parent and child coefficients, the parameters of the child coefficients can be estimated with the aid of a MAP filter. Let 1x_r be the detail coefficient considered and 2x_r its parent (the detail coefficient situated in the same position but computed in the next iteration). It can be seen analyzing figure 4 that a parent coefficient corresponds to four child coefficients. This is the reason why each image containing parent coefficients will be over-sampled to have the same number of coefficients like the corresponding child coefficients sub-image. Then the statistical parameters of the child coefficients will be determined using the parent coefficients situated in the same position and the neighbor detail coefficients, situated into a rectangular window centered on the current child coefficient. It can be written:

$${}^1x_r = {}^1s_r + {}^1b_r, \quad (28)$$

and :

$${}^2x_r = {}^2s_r + {}^2b_r, \quad (29)$$

or:

$$\mathbf{x}_r = \mathbf{s}_r + \mathbf{b}_r, \quad (30)$$

where the following notations were used :

$$\mathbf{x}_r = ({}^1x_r, {}^2x_r), \quad \mathbf{s}_r = ({}^1s_r, {}^2s_r), \quad \mathbf{b}_r = ({}^1b_r, {}^2b_r). \quad (31)$$

The MAP estimation of \mathbf{s}_r using the observation \mathbf{x}_r is given by:

$$\hat{\mathbf{s}}_r(\mathbf{x}_r) = \underset{\mathbf{s}_r}{\operatorname{argmax}} \{ \ln(p_{\mathbf{b}_r}(\mathbf{x}_r - \mathbf{s}_r) \cdot p_{\mathbf{s}_r}(\mathbf{s}_r)) \} \quad (32)$$

Making the hypothesis verified (at high scales) that the model of the image \mathbf{b}_r (corresponding to the WT of the noise) is a zero mean Gaussian white noise, it can be written:

$$p_{\mathbf{b}_r}(\mathbf{b}_r) = \frac{1}{2\pi\sigma_b^2} e^{-\frac{{}^1b_r^2 + {}^2b_r^2}{2\sigma_b^2}}. \quad (33)$$

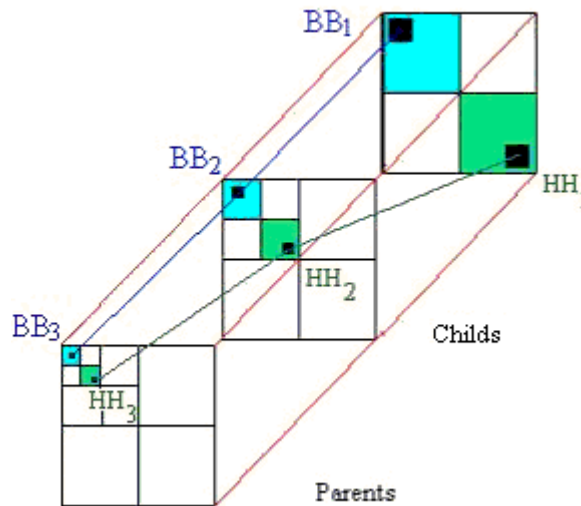


Figure 4. The dependency across the scales of the DWT coefficients. For example, the parents of the coefficients from the HH_2 sub-image belong to the HH_3 sub-image.

For the WT of the useful part of the input image, in [7] is proposed the following model:

$$p_{s_r}(s_r) = \frac{3}{2\pi\sigma^2} e^{-\frac{\sqrt{3}}{\sigma} \sqrt{({}^1s_r)^2 + ({}^2s_r)^2}}, \quad (34)$$

where 1s_r represents the set of coefficients of the m 'th iteration of the DWT of the useful image and 2s_r represents the set of coefficients of the next iteration of the same DWT.

With the aid of the notation $f(s_r) = \ln(p_{s_r}(s_r))$, the MAP filter equation, with the pdfs defined in relations (33) and (34), can be written in the following form:

$$\hat{s}_r(x_r) = \operatorname{argmax}_{s_r} \left\{ -\frac{({}^1x_r - {}^1s_r)^2}{2\sigma_b^2} - \frac{({}^2x_r - {}^2s_r)^2}{2\sigma_b^2} + f(s_r) \right\}, \quad (35)$$

equivalent to the following system of equations:

$$\begin{cases} \frac{{}^1x_r - {}^1\hat{s}_r}{\sigma_b^2} + \frac{\partial f}{\partial {}^1s_r}(s_r) = 0 \\ \frac{{}^2x_r - {}^2\hat{s}_r}{\sigma_b^2} + \frac{\partial f}{\partial {}^2s_r}(s_r) = 0 \end{cases} \quad (36)$$

Hence:

$$\begin{cases} \frac{{}^1x_r - {}^1\hat{s}_r}{\sigma_b^2} + f_1(s_r) = 0 \\ \frac{{}^2x_r - {}^2\hat{s}_r}{\sigma_b^2} + f_2(s_r) = 0 \end{cases} \quad (37)$$

Taking into account the definition of the function f :

$$f(s_r) = \ln(p_{s_r}(s_r)), \quad (38)$$

and the expression of the pdf from (34), the last system of equations takes the form:

$$\begin{cases} \frac{{}^1\hat{s}_r - {}^1x_r}{\sigma_b^2} - \frac{\sqrt{3}}{\sigma} \frac{{}^1\hat{s}_r}{\sqrt{({}^1x_r)^2 + ({}^2x_r)^2}} = 0 \\ \frac{{}^2\hat{s}_r - {}^2x_r}{\sigma_b^2} - \frac{\sqrt{3}}{\sigma} \frac{{}^2\hat{s}_r}{\sqrt{({}^1x_r)^2 + ({}^2x_r)^2}} = 0 \end{cases} \quad (39)$$

The first solution of this system is:

$${}^1\hat{s}_r = \frac{\left(\sqrt{({}^1x_r)^2 + ({}^2x_r)^2} - \frac{\sqrt{3}\sigma_b^2}{\sigma} \right)_+}{\sqrt{({}^1x_r)^2 + ({}^2x_r)^2}} \cdot {}^1x_r, \quad (40)$$

where:

$$(g)_+ = \begin{cases} g & \text{for } g > 0 \\ 0 & \text{otherwise.} \end{cases} \quad (41)$$

The variance σ_b can be estimated using the following relation:

$$\hat{\sigma}_b^2 = \frac{\text{median}(|x_r(n, p)|)}{0.6745} \quad (n, p) \in D_1^3. \quad (42)$$

For the estimation of σ , the local variance of the useful part of the input image, the following relations can be used. First, the local mean of the acquired image is estimated:

$$\hat{m}_{x_r}[n, p] = \frac{1}{(2P+1)^2} \sum_{(k,l) \in F_{n,p}} x_r[k, l] \quad (43)$$

where, $F_{n,p}$ represents a rectangular moving window with dimensions $(2P+1) \times (2P+1)$ centered on the current coefficient. Second, the local variance of the input image is estimated with the aid of the following relation:

$$\hat{\sigma}_{x_r}[n, p] = \frac{1}{(2P+1)^2} \sum_{(k,l) \in F_{n,p}} (x_r[k, l] - \hat{m}_{x_r}[n, p])^2. \quad (44)$$

Using these values, the local variance of the useful part of the input image can be computed with the aid of the following relation:

$$\hat{\sigma}^2[n, p] = \max(0, \hat{\sigma}_{x_r}^2[n, p] - \hat{\sigma}_b^2). \quad (45)$$

3.3.2. Statistical analysis

Analyzing the relation (40), the perfect symmetry of the bishrink filter input-output relation can be remarked. It transforms a zero mean constant image into another zero mean constant image. All the detail sub-images are zero mean. The mean of the approximation sub-image is not null, but this sub-image is not filtered. So, the bishrink filter is an estimator unbiased. The mean of the speckle noise is equal with 1 but the mean of the logarithm of the speckle $\mu_{\log-\Gamma}$ is not null. So, the first block in figure 1 affects the mean of the acquired image. This is the reason why the mean compensation technique, presented in figure 1, must be applied. The mean of the acquired image i_r is equal with the mean of its useful component i_o , because $\mu_\Gamma = 1$. So the mean extraction block from figure 1 computes the mean of i_o . The mean compensation block computes the mean of the image obtained after the logarithm inversion, subtracts it and adds the mean of i_o , furnished by the mean extraction block. The relation (40) can be put in the following form:

$$({}^1\hat{s}_r)^2 = \begin{cases} \left(\frac{\sqrt{({}^1x_r)^2 + ({}^2x_r)^2} - \sqrt{3}\sigma_b^2}{\sigma} \right) \cdot ({}^1x_r)^2 & \text{if } \sqrt{({}^1x_r)^2 + ({}^2x_r)^2} > \frac{\sqrt{3}\sigma_b^2}{\sigma}, \\ 0, & \text{otherwise} \end{cases}$$

or:

$$({}^1\hat{s}_r)^2 = \begin{cases} ({}^1x_r)^2 & \text{if } \sqrt{({}^1x_r)^2 + ({}^2x_r)^2} > \frac{\sqrt{3}\sigma_b^2}{\sigma}. \\ 0, & \text{otherwise} \end{cases}$$

Computing the statistical mean of the two sides in the last relation it can be written:

$$\sigma_{1\hat{s}_r}^2 \leq \sigma_{1x_r}^2.$$

The bishrink filter is a performing estimator. For the computation of the IDTDWT, two IDWT must be used. This is a source for a further reduction of the noise variance.

3.4. A comparison of different filters

To highlight the advantages of the association between the DTDWT and the bishrink filter, some results are presented in the table 1. Different WTs are associated with different filters. The following WTs are used: the DWT, the DEDWT, [11], [12] and the DTDWT. We have used in the domain of those WTs the following filters: the zero order Wiener filter, the second order Wiener filter, the hard thresholding and the soft thresholding filters and the bishrink filter. For every experiment the Lena test image was used. It was perturbed by an additive white Gaussian noise with different variances (presented in the first column of the table). The different simulation results are compared using the pick signal to noise ratios, PSNRs, obtained. The expression of this quantity is the following:

$$PSNR = 20 \log_{10} \frac{256}{\sqrt{mse}},$$

where mse represents the mean square error of the estimation.

Each time the DWTs corresponding to the nine Daubechies' mother wavelets, having a number of vanishing moments between 2 and 10 and minimum support, are computed. These results are used for the comparison of the denoising methods based on DWT and for the computation of the DEDWT. The DTDWT is also computed, when the bishrink filter is analyzed. After the application of a filtering method, the computation of the corresponding IWT is performed and the PSNR is obtained. The better result obtained using the DWT can be found on the first sub-column of each column in the table. The mother wavelets used to obtain those results are also specified in the same sub-column. In the second sub-column of each column allocated to a filter are specified the PSNRs obtained using the DEDWT. This way the effect of the association of the corresponding filtering method with the better DWT can be compared with the effect of the association of that filtering method with the DEDWT.

For the bishrink filter case, the DTDWT is also considered. The PSNRs obtained using this transform are specified in the third sub-column of the last column.

The zero order Wiener filter impulse response is, [13]:

$$\hat{h}_{n,p}[x,y] = \frac{\hat{\sigma}^2[n,p]}{\hat{\sigma}^2[n,p] + \hat{\sigma}_b^2} \cdot \delta[x,y].$$

The noise variance is estimated using the relation (42). The useful component local variance is estimated using the relations (43), (44) and (45) and a 3x3 moving window, $F_{n,p}$. The results obtained are presented in the third column of the table.

The second order Wiener filter uses the following model for the correlation function of a real image:

$${}_{(n,p)}\Gamma_s[k,l] = \begin{cases} r_{0,0} \cdot \rho^{|k|+|l|}, & (k,l) \in F_{n,p} \\ 0, & |k| > nP \text{ or } |l| > nP \end{cases}$$

This model, for $\rho < 1$, considers that the influence of the central pixel on the other pixels in the window decreases when the distance between those pixels increases. The decreasing speed depends on the value of ρ .

The value $r_{0,0}$ is given by $\hat{\sigma}^2[n,p]$. The impulse response of the second order Wiener filter, $h(p,q)$ is given by the following system of equations:

$$\begin{bmatrix} h(1,1) \\ h(1,0) \\ h(0,1) \\ h(0,0) \end{bmatrix} = \begin{bmatrix} r_{0,0} + \sigma_b^2 & r_{0,0} \cdot \rho & r_{0,0} \cdot \rho & r_{0,0} \cdot \rho^2 \\ r_{0,0} \cdot \rho & r_{0,0} + \sigma_b^2 & r_{0,0} \cdot \rho & r_{0,0} \cdot \rho \\ r_{0,0} \cdot \rho & r_{0,0} \cdot \rho & r_{0,0} + \sigma_b^2 & r_{0,0} \cdot \rho \\ r_{0,0} \cdot \rho^2 & r_{0,0} \cdot \rho & r_{0,0} \cdot \rho & r_{0,0} + \sigma_b^2 \end{bmatrix}^{-1} \begin{bmatrix} r_{0,0} \cdot \rho^2 \\ r_{0,0} \cdot \rho \\ r_{0,0} \cdot \rho \\ r_{0,0} \end{bmatrix}.$$

The results obtained using this filter are presented in the forth column of the table for $\rho = 0.7$.

The soft-thresholding filter is a non-linear one and has the following input-output relation:

$$\text{soft}(g, \tau) = \text{sgn}(g) (|g| - \tau)_+.$$

If the threshold τ is selected proportional with the variance of the input noise then this filter is an adaptive one, [10]. The constant of proportionality takes different values according to different cost functions. For the case when the Min-Max approximation error must be minimized, the value of the constant of proportionality is of $\sqrt{2 \ln N}$, where N represents the number of pixels of the input image. Another value of the constant of proportionality, corresponding to the cost functional given by the power of the output noise is 3 (taking into account the rule of three sigmas, that can be applied in the case of a Gaussian pdf). In our case the value of the output PSNR must be maximized. This is the reason why we have repeated the experiments associated with the soft thresholding filter many times for each mother wavelets, each time using another constant of proportionality and we have selected the constant corresponding to the maximum output PSNR. The results obtained using the soft-thresholding filter are presented in the fifth column of the table.

The input-output relation of the hard-thresholding filter is:

Table 1. A comparison of different denoising methods. The case of additive noise.

σ_b	Noisy	Zero order Wiener Filter		Second order Wiener filter		Soft thresholding		Hard thresholding		Bishrink		
		Best DWT	DE DWT	Best DWT	DE DWT	Best DWT	DE DWT	Best DWT	DE DWT	Best DWT	DE DWT	DT DWT
10	28.1	D5 32.6	32.9	D 6 31.9	32.4	D 4 31.0	31.8	D 5 30.8	33.4	D 6 34.2	35.0	35.3
15	24.6	D9 29.5	29.6	D6 29.2	29.7	D5 28.9	29.8	D 5 28.2	30.9	D 6 32.3	33.1	33.7
20	22.1	D 10 27.3	27.3	D 6 27.3	27.7	D 5 27.2	28.1	D 4 26.6	29.1	D 5 31.0	31.8	32.4
25	20.2	D 9 25.4	25.5	D 4 25.7	26.0	D 6 25.9	26.9	D 5 25.4	27.8	D 5 29.8	30.7	31.4
30	18.6	D 6 24.0	24.0	D7 24.4	24.6	D5 25.0	25.9	D 6 24.5	26.7	D 5 29.0	29.8	30.5
35	17.3	D 4 22.6	22.6	23.3	23.6	D 5 24.2	25.2	D 6 23.7	25.8	D 5 28.3	29.1	29.8

$$\text{hard}(g, \tau) = \begin{cases} g, & |g| > \tau \\ 0, & \text{elsewhere} \end{cases}.$$

The same threshold selection method was used. The results obtained are presented in the sixth column of the table. In the last column, the results obtained with the bishrink filter are presented.

Some remarks can be done, analyzing the table:

- R1. The results obtained using the DEDWT are always superior to the results obtained using the best DWT. The idea to enhance the diversity of the mother wavelets from the Daubechies' family improves the performances of any denoising method.
- R2. The bishrink filter is the best. Its superiority is explained by the fact that it takes into account the inter scale dependency of the wavelet coefficients. It is superior versus the Donoho's hard thresholding or soft thresholding filters. The reason is that for the threshold selection, in the case of Donoho's filters, only the noise is considered (the wavelet coefficients of the useful part of the processed image are not

taken into account). The Donoho's filters are superior versus the Wiener filters, especially when the noise variance is high. In fact, the zero order Wiener filter is a MAP filter. It represents the solution to the problem described in (32) when the pdf of the wavelet coefficients of the useful part of the input image is considered Gaussian. This is the reason why we can consider that the hypothesis described in (34) (the Laplace distribution, a heavy tailed one) is superior to the Gaussian hypothesis. For the bishrink filter, the gain increasing associated to the use of the DEDWT is of 0.8 dB versus the use of the best DWT.

- R3. The denoising method based on the association of the DTDWT with the bishrink filter is the best between the methods compared in table 1.

Next, some classical methods for the reduction of the speckle noise are compared with the method proposed in this paper. These methods are based on different filter types: moving averager, median, Lee, Kuan, Gamma and Frost. The use of those filters represents classical SONAR images denoising solutions. The same synthetic image (like in the case of experiments presented in table 1), Lena, was corrupted this time, with a multiplicative noise of Rayleigh type. The mean square error of the noisy image is of 3635. In table 2 are presented the mean square errors obtained after the denoising realized with each filter. These filters have some specific parameters, like the dimension of the moving window used, or the number of times the filter is applied in the processing of the same input image. The best moving averager for the treatment of the considered noisy image is that having a window of dimensions 5x5. From the family of median filters, the best for our treatment is that which uses a moving window of dimensions 7x7. For the families of Lee's filters, Kuan's filters, Gamma filters and Frost's filters, there are three parameters that can be selected: the dimensions of the moving window, a value called the filter's parameter and the number of times the filter is applied, [14]. The best Gamma filter, for the treatment of the considered image, corresponds to the following parameters' values: 5x5, 1.5 and 1. Finally the parameter values of the best Frost's filter are: 5x5, 1 and 1.

Table 2. A comparison of different denoising methods. The case of multiplicative noise.

Noisy Image	Moving Averager 5	Median Filter 7	Lee's Filter 7-5-1	Kuan's Filter 9-5- 5-1	Gamma Filter 5- 1.5- 1	Frost's Filter 5-1-1	Bishrink+ DEDWT	Bishrink+ DTDWT
3635	571.7	569.8	807.5	732.8	559.5	566	301.4	250.3

4. REAL DATA PROCESSING RESULTS

The image presented in figure 5 is the original SONAR image. It can be seen that the speckle is fully developed. The result obtained, using the proposed denoising method (DTDWT + bishrink), is presented in figure 6. Analyzing the two images, it can be observed the fact that the noise was practically entirely removed and the fact that the details of the useful part of the input image (textures or edges) were not affected by the treatment proposed. More, some hidden details can be observed in figure 6. An objective measure of the performances of a denoising method for SONAR images is the enhancement of the Equivalent Number of Looks, ENL. This is a measure of the performances obtained in homogenous zones. The ENL is defined with the following relation:

$$ENL = \left(\frac{\text{mean}}{\text{standard deviation}} \right)^2$$

The ENLs of the images presented in figures 5 and 6 are computed in the same homogenous zone of dimensions 128x128, localized in the right up corner. The value obtained for the image in figure 5 is of 7.34 and the value obtained for the image in figure 6 is of 76.64. So, the proposed denoising method enhances more than ten times the ENL. Comparing the two images, it can be observed the good conservation of the mean of the useful part of the input image. Of course, the whole treatment can be enhanced if a de-blurring method is also applied. The result from figure 6 was obtained computing four iterations of the DTDWT. This value represents a superior bound of the iterations number for an image with 1024x1024 pixels when the bishrink filter is used, taking into account the estimations described by the relations (42)-(45). For a higher iterations number, the quality of those approximations decreases due to the increasing of the estimation

errors (insufficient statistics). The moving window used for the bishrink filtering had dimensions 7×7 . The good quality of the image from figure 6 proves the validity of the theoretical results presented in the previous paragraphs.

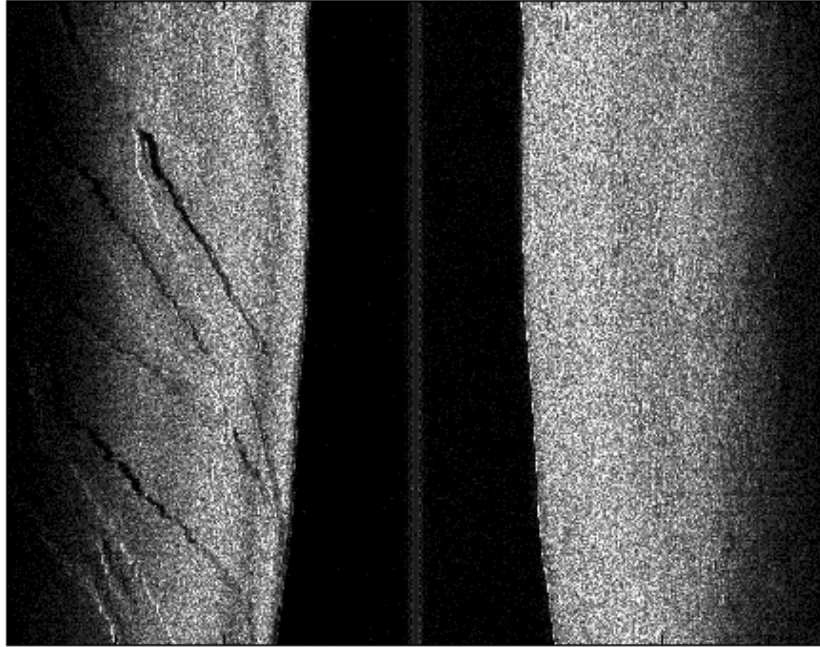


Figure 5. The SONAR image to be denoised, representing a zone of sea floor. The speckle is fully developed. An IFREMER team acquired the image during a campaign on the Atlantic Ocean. The permission to use this image is granted to our research team.



Figure 6. The result obtained. The noise was practically entirely removed and the details of the useful part of the input image (textures or edges) were not affected by the treatment proposed. Some hidden details can be observed.

5. CONCLUSION

A new denoising method for the processing of SONAR images was proposed. It is based on the use of the DTCWT. This method combines image multiscale analysis and classical techniques of adaptive filtering. It permits to retain coefficients produced by significant structures present in the useful part of the input image and suppresses those produced by the speckle noise. A complete statistical analysis of this method was reported. Simulations confirmed the hypotheses and the results of this statistical analysis. The wavelet coefficients correlation analysis is original. From $\log\text{-}\hat{A}^2$ assumptions for the pdf of the reflectivity and of the speckle, we have expressed the pdf of the wavelet coefficients. This is a heavy-tailed distribution. We have approximated this distribution with a Laplace pdf. Using this hypothesis a MAP filter with closed-form input output relation was derived. Its parameters are locally estimated. In this estimation process a very important property of the WTs, the correlation between wavelet coefficients at the same position and successive scales, is exploited. An adaptive mean correction method was also proposed. We evaluated the results on both synthetic data and real SONAR images, validating the theoretical hypotheses used. Further improvements could be obtained if a better WT and a 3D bishrink filter would be used. This latter avenue is currently under investigation and results will be reported soon.

ACKNOWLEDGMENTS

The research with the results reported in this paper was realized in the framework of the Programme de recherche franco-roumain Brancusi with the title: Débruitage des images SONAR en utilisant la théorie des ondelettes: applications aux systèmes d'aide à la décision pour la classification, directed by the associated professor Sorin Moga from ENST-Bretagne, Brest, France. It is also the result of many fruitful discussions with Xavier Lurton, Jean-Marie Augustin and Ronan Fablet, specialists from IFREMER Brest and with Michel Legris, researcher and teacher at ENSIETA Brest. The authors are grateful to the IFREMER specialists for the permission to treat the image in figure 5.

REFERENCES

1. FJØRTOFT R., LOPÈS A., ADRAGNA F., *Radiometric and Spatial Aspects of Speckle Filtering*, Proc. IGARSS'2000, Honolulu, Hawaii, July 24-28, 2000.
2. GAGNON L., *Wavelet Filtering of Speckle Noise-Some Numerical Results*, Proceedings of the conference Vision Interface 1999, Trois Riviers, Canada, 1999.
3. WALESSA M., DATCU M., *Model-Based Despeckling and Information Extraction from SAR Images*, IEEE Trans. on Geosciences and Remote Sensing, **38**, 5, 2258-2269, 2000.
4. FOUCHER S., BENIE G. B., BOUCHER J.-M., *Multiscale MAP Filtering of SAR images*, IEEE Transactions on Image Processing, **10**, 1, 49-60, 2001.
5. ISAR D., ISAR A., MOGA S., LURTON X., AUGUSTIN J.-M., *Multi-scale MAP Despeckling of SONAR Images*, Proceedings of IEEE International Conference Oceans'05, Brest, France, June 20-23, 2005.
6. KINGSBURY N., *Complex Wavelets for Shift Invariant Analysis and Filtering of Signals*, Applied and Computational Harmonic Analysis **10**, 2001, 234-253.
7. SENDUR L., SELESNICK I. W., *Bivariate shrinkage functions for wavelet-based denoising exploiting interscale dependency*. IEEE Trans. on Signal Processing. **50**, 11, 2744-2756, 2002.
8. DAUBECHIES I., *Ten Lectures on Wavelets*, CBMS-NSF Reg. Conf. Series in Appl. Math., SIAM, Philadelphia, PA. 1992.
9. ISAR A., MOGA S., LURTON X., *A Statistical Analysis of the 2D Discrete Wavelet Transform*, Proceedings of the International Conference AMSDA 2005, May, 17-20, 2005, 1275-1281.
10. DONOHO D. L., JOHNSTONE I. M., *Ideal spatial adaptation by wavelet shrinkage*, Biometrika, **81**, 3, 425-455, 1994.
11. ISAR A., ISAR D., *A New Discrete Wavelet Transform*, Revue roumaine des sciences techniques, serie Électrotechn. et energetique, **47**, 3, 2002, 411-415.
12. ISAR A., QUINQUIS A., LEGRIS M., ISAR D., *Débruitage des images SAR: Application de la TODDE (Transformée en Ondelettes Discrète à Diversité enrichie)*, Revue scientifique et technique de la défense, **64**, 139-148, 2004.
13. ZHANG H., NOSTRATINIA A., WELLS JR. R. O., *Image Denoising via Wavelet-Domain Spatially Adaptive FIR Wiener Filtering*, Proceedings of IEEE ICASP, Istanbul, June 2000, vol. 5, 2179-2182.
14. GILGENKRANTZ E., *Etude quantitative de quelques filtres anti-speckle*, Master Thesis realized under the coordination of Michel Legris, ENSIETA Brest 2002.